Article

Chinese Science Bulletin

SPECIAL TOPIC
Bio-spectroscopic Sensing

November 2011 Vol.56 No.31: 3260–3265
doi: 10.1007/s11434-011-4662-1

A near-infrared fluorescent probe for fluorine ions and its application in the imaging of HepG2 cells

GONG Wei, SU RuiXian, LI Lu, XU KeHua & TANG Bo*

Key Laboratory of Molecular and Nano Probes of Ministry of Education, Engineering Research Center of Pesticide and Medicine Intermediate Clean Production of Ministry of Education, College of Chemistry, Chemical Engineering and Materials Science, Shandong Normal University, Jinan 250014, China

Received February 23, 2011; accepted March 8, 2011

In this study, we have designed and synthesized a new near-infrared (NIR) fluorescent probe (BODIPY-Se) to detect fluorine ions (F^-) using a B-Se bond to connect the fluorescent dye BODIPY and benzotrifluoride. The probe exhibited a highly selective fluorescence response to F^- with a detection limit of 7.4×10^{-8} mol/L. The excitation and emission spectra of the probe in the NIR region avoid background fluorescence interference present in biological systems. The fluorescent imaging of HepG2 cells demonstrated that the newly developed probe should be broadly applicable to detect F^- in living cells.

near infrared, fluorescent probe, fluorine ion, BODIPY

Citation: Gong W, Su R X, Li L, et al. A near-infrared fluorescent probe for fluorine ions and its application in the imaging of HepG2 cells. Chinese Sci Bull, 2011, 56: 3260–3265, doi: 10.1007/s11434-011-4662-1

F^-, the smallest anion, is an indispensable trace element for the survival of organisms. Appropriate amounts of fluoride can be used in osteoporosis treatment [1–3] and the prevention of dental caries [4]. However, excess F^- results in fluorosis and renal, gastrointestinal and immunological toxicity [5], such as dental fluorosis, crippling fluorosis, impairment of the immune system, inhibition of key enzymes, neurotoxicity and a reduction in IQ [6]. In addition, fluoride causes changes in collagen and the metabolism of glycosaminoglycans (GAG), the main substance of connective tissue [7]. Although, the structural chemistry of fluoride is well understood, many questions related to fluoride homeostasis and its action in biological systems remain unanswered. It is appealing to make fluoride "visible" in tissues and even in living cells.

Therefore, there is a need to develop highly sensitive and specific fluorescent probes that can be applied in the detection of cellular F^-. Several types of molecular probes have been reported for fluoride detection, including probes that hydrogen bond between the N–H of a urea or pyrrole group and the fluoride ion [8,9]. Solvent effects play a crucial role in controlling the binding strength and selectivity for F^-. On the other hand, there have been a few reports regarding F^- detection using unique fluoride-boron [10–19] and fluoride-silica [20–22] interactions. To improve the sensitivity of the fluoride-induced-lactonization detection scheme, a semiconductor polymer that amplifies the response has been proposed [22]. However, this polymer is essentially membrane impermeable thereby making it unsuitable for monitoring intracellular fluoride levels.

Many BODIPY products involving the substitution of fluorine have been synthesized in recent years [23–27]. Using this strategy, one of the fluorine atoms on the BODIPY dye is replaced with a selenium atom. Using a B–Se bond to connect BODIPY and benzotrifluoride, a near-infrared probe BODIPY-Se was successfully synthesized. The fluorescence is quenched because of photoinduced electron transfer (PET). The B–Se bond of the probe is cleaved when reacting with the nucleophilic F^- to yield BODIPY (Scheme 1). Here, we report the design, synthesis, and application of

*Corresponding author (email: chemtangb@yahoo.cn)

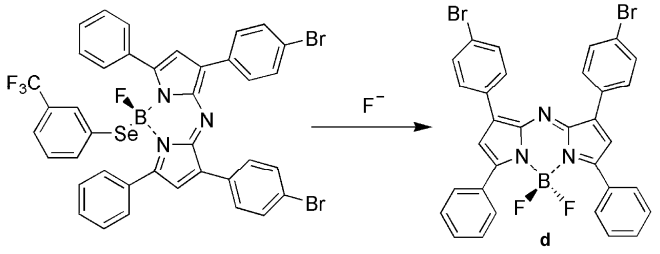

Scheme 1 The reaction of BODIPY-Se with a fluorine ion.

the novel NIR fluorescent probe for F^- detection. The results show that the probe has excellent selectivity and sensitivity. The imaging of F^- in living cells indicates that the developed probe should be useful for high-throughput F^- screening in living cells.

1 Experimental

1.1 Materials and apparatus

m-Trifluoromethylphenyl bromide was purchased from Alfa Aesar. All other chemicals were obtained from standard reagent suppliers and of analytical-reagent grade. Ultrapure water (18.2 MΩ cm) was used throughout and obtained from an ultrapurification system (Sartorius, Göttingen, Germany). Fluorescence spectra were obtained with an FLS-920 fluorescence spectrometer (Edinburgh, England) with a xenon lamp and 1.0-cm quartz cells with slits of 2.5/2.5 nm. All pH values were measured with a pH-3*c* digital pH-meter (PB-21, Sartorius, Göttingen, Germany). ^{1}H NMR spectra were acquired on an AVANCE 300 spectrometer (Bruker, Switzerland). The fluorescence images of the cells were taken using a confocal laser scanning microscope (TCS SPE, Leica, Wetzlar, Germany) with an objective lens (×40) and the excitation wavelength was 633 nm (10 mW).

1.2 Synthesis of the fluorescent probe

(i) Synthesis of BODIPY. The synthetic route of BODIPY is shown in Scheme 2. The main products were characterized by NMR spectroscopy.

Synthesis of 3-(4-bromo-phenyl)-1-phenyl-propenone (**a**): 4-bromobenzaldehyde (3.7 g, 20 mmol), acetophenone (2.8 g, 23 mmol) and sodium hydroxide (2.0 g) were dissolved in 23 mL H_2O and 40 mL ethanol, and the mixture was stirred at room temperature for 24 h. During the course of the reaction, the product precipitated from the reaction mixture. After filtration, the product was obtained as a yellow solid. m.p. 117–119°C; ^{1}H NMR (300 MHz, $CDCl_3$) δ 8.03–8.01 (d, 2H), 7.78–7.72 (d, 1H), 7.48–7.61 (m, 8H); IR (KBr disc) cm^{-1}: 1658.

Synthesis of 3-(4-bromophenyl)-4-nitro-1-phenyl-butan-1-one (**b**): **a**(8.0 g, 28 mmol), nitromethane (9.6 g) and diethylamine (8.0 mL) were dissolved in dry methanol (100 mL) and heated under reflux for 24 h. The solution was cooled, acidified with 1 mol/L HCl and the resulting precipitate was isolated by filtration. The product **b** was obtained as a yellow solid. m.p. 90–92°C; ^{1}H NMR (300 MHz, $CDCl_3$) δ 7.93–7.90 (d, 2H), 7.62–7.57 (m, 1H), 7.47–7.45 (m, 4H), 7.11–7.19 (m, 2H), 4.83–4.53 (m, 2H), 4.26–4.19 (m, 1H), 3.49–3.42 (m, 2H); IR (KBr disc) cm^{-1}: 1684.

Synthesis of [3-(4-bromophenyl)-5-phenyl-1*H*-pyrrol-2-yl][3-(4-bromophenyl)-5-phenylpyrrol-2-ylidene] amine (**c**): **b**(3.0 g, 8.6 mmol) and ammonium acetate (23 g) were dissolved in ethanol (100 mL) and heated under reflux for 48 h. The reaction was cooled to room temperature, the solvent was concentrated to 20 mL and filtered, and the isolated solid was washed with ethanol to yield the product **c** as a purple solid.

Synthesis of the BF_2 chelate of [3-(4-bromophenyl)-5-phenyl-1*H*-pyrrol-2-yl][3-(4-bromophenyl)-5-phenylpyrrol-2-ylidene]amine (**d**): **c**(0.47 g, 0.77 mmol) was dissolved in dry CH_2Cl_2 (150 mL), treated with triethylamine (4 mL) and boron trifluoride diethyl etherate (2 mL), and stirred at room temperature under Ar for 36 h. The mixture was washed with water. Purification by column chromatography on silica eluting with CH_2Cl_2/petroleum ether (2∶3) gave the product **d** as a metallic brown solid**.** ^{1}H NMR (300 MHz, $CDCl_3$) δ 8.04 (m, 4H), 7.93–7.91 (d, 4H), 7.64–7.60 (d,

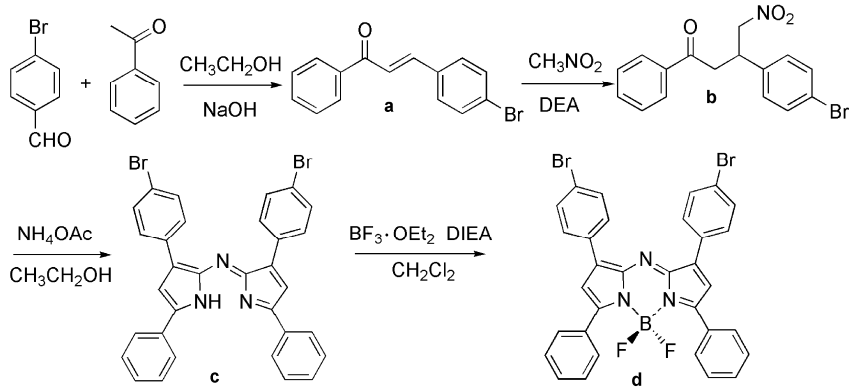

Scheme 2 Synthetic route of BODIPY.

4H), 7.51–7.53 (m, 6H), 7.04 (s, 2H); IR (KBr) cm^{-1}: 1543.

(ii) Synthesis of the fluorescent probe. The synthetic route of BODIPY-Se is shown in Scheme 3.

Synthesis of 3,3′-bis(trifluoromethyl) diphenyl diselenide (**e**): A three-neck round-bottomed flask was fitted with a reflux condenser, a dropping funnel and an argon inlet tube. M-trifluoromethylphenyl magnesium bromide was prepared using 2.7 mL (19.5 mmol) of *m*-bromobenzotrifluoride, 0.48 g (25 mmol) of magnesium turnings, and 20 mL of dry tetrahydrofuran. After stirring for 2 h at room temperature, 1.52 g (19.3 mmol) of powdered black selenium was added gradually over a 10 min period through the side arm. It is important to avoid the introduction of oxygen during this operation. After stirring for an additional 4 h, 20 g of ice was slowly added to the flask followed by 4 mL of concentrated HCl and 20 mL of methanol. Air was bubbled through the sample for 24 h. The mixture was treated with a separatory funnel and the organic phase was treated by removing the solvent in vacuo. Distillation of the residue gave the diselenide product as an orange liquid. ^{1}H NMR (300 MHz, $CDCl_3$) δ 7.91 (s, 2H), 7.80–7.78 (d, 2H), 7.54–7.52 (d, 2H), 7.41–7.39 (q, 2H).

Synthesis of 3-trifluoromethyl diphenyl selenol (**f**): **e** (0.224 g, 0.5 mmol) was dissolved in 6 mL of ethanol which contained 0.02 g NaOH and was stirred at 0°C. Subsequently, 0.038 g (10 mmol) $NaBH_4$ was added while stirring the reaction mixture. The mixture was allowed to reach room temperature, during which the color of the solution changed from orange to colorless. Concentrated HCl was added until the pH reached 6–7 and the mixture was cooled to 0°C. The mixture was treated with a separatory funnel and the organic phase was treated by removing the solvent in vacuo.

Synthesis of BODIPY-Se: A three-neck round-bottomed flask was fitted with a reflux condenser and an argon inlet tube. Selenol (**f**) and 18 mg (0.75 mmol) sodium hydride was dissolved in 6 mL of CH_2Cl_2. After stirring for 2 h at room temperature, 0.05 g BODIPY was added gradually and the solution was stirred for an additional 12 h at 40°C. Purification by column chromatography on silica eluting with CH_2Cl_2/petroleum ether (3∶1) gave the product BODIPY-Se as a green solid. ^{1}H NMR (300 MHz, $CDCl_3$) δ 8.49 (m, 2H), 8.11 (m, 2H), 7.95–7.92 (d, 2H), 7.64–7.59 (m, 8H), 7.48 (d, 4H), 7.42 (d, 4H), 7.32 (s, 2H).

1.3 Cell culture and confocal imaging

The human hepatoma cell line (HepG2) was first grown in a circular petri dish (60 mm) using RPMI 1640 medium supplemented with 10% fetal bovine serum (FBS), $NaHCO_3$ (2 g/L) and 1% antibiotics (penicillin/streptomycin, 100 U/mL). When the cells reached 80% confluence, they were transferred from the petri dish and cultured directly on sterile coverslips, which were rinsed and dried in a circular petri dish (35 mm). The cells (0.1 mL, 1×10^6 cells/mL) were carefully added onto each coverslip to ensure uniform coverage and allowed to adhere onto the coverslips. The same cell medium was then added to cover the coverslips in petri dishes, which were placed in a CO_2 incubator and maintained under the same conditions for 24 h. The cells were incubated with or without F^- (1.0 μmol/L) for 1 h and 1.0 μmol/L probe was subsequently added and the cells were incubated for 1 h. Before the imaging was performed, the cells were washed with PBS three times after the original medium had been removed. Confocal fluorescence images were obtained on a confocal laser scanning microscope with an objective lens (×40). The excitation wavelength was 633 nm.

2 Results and discussion

2.1 Spectra properties

The spectral properties of BODIPY-Se were tested. Figure 1 shows the excitation and emission spectra of BODIPY-Se before and after its reaction with F^- in PBS buffer. A noticeable increase of the fluorescence intensity appeared after the probe reacted with F^-. The fluorescence spectra, λ_{max}, of the excitation and emission of BODIPY-Se are positioned at 660 and 690 nm respectively. These wavelengths should effectively avoid background fluorescence interference arising from biological systems.

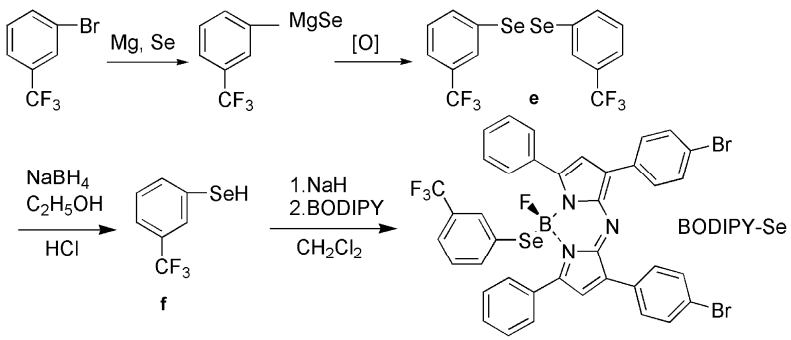

Scheme 3 Synthetic route of BODIPY-Se.

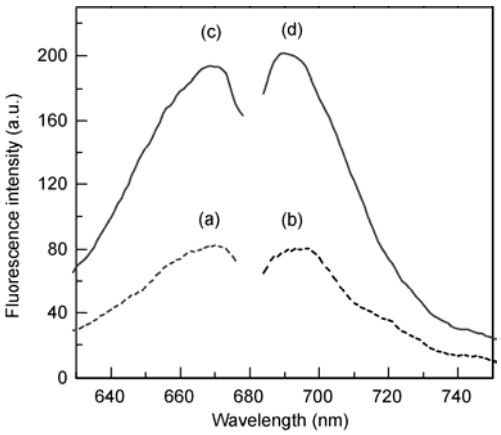

Figure 1 Excitation and emission spectra of BODIPY-Se before and after its reaction with F^-. (a) and (b) are the excitation and emission spectra of BODIPY-Se before its reaction with F^-, respectively. (c) and (d) are the excitation and emission spectra of BODIPY-Se after its reaction with F^-, respectively. $\lambda_{ex(a, c)} = 660$ nm, $\lambda_{em(b, d)} = 690$ nm.

2.2 Optimization of the experimental variables

To optimize detection, the effects of particular experimental variables were determined during the reaction of BODIPY-Se and F^-.

(i) Effect of pH. In the experiment, the pH of the medium has a significant effect on the fluorescence intensity of the probe. The fluorescence intensity was detected in the PBS buffer with different pH values. As shown in Figure 2, pH 7.4 was appropriate to detect F^-. To obtain higher signal-to-noise values, PBS buffer (pH 7.4, which matches physiological conditions) was employed throughout the analytical experiments.

(ii) Effect of the PBS concentration. The effect of the PBS concentration was examined. As show in Figure 3, the fluorescence intensity reached a maximum intensity at 5.0 mmol/L. Consequently, 5.0 mmol/L PBS was considered suitable for the experiments.

(iii) Effect of probe concentration. The accuracy and sensitivity was also affected by the concentration of the probe. The results presented in Figure 4 show that when probe concentration was less than 1.0 μmol/L, the fluorescence intensity increased with increasing concentration of the probe. The fluorescence intensity reached a maximum when the probe concentration ranged between 1.0 to 1.2 μmol/L, and the intensity decreased at probe concentrations > 1.2 μmol/L. Thus, a probe concentration of 1.0 μmol/L was used in the experiments.

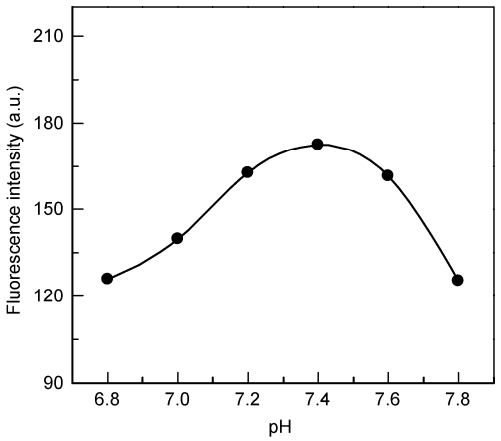

Figure 2 The effect of pH on the fluorescence intensity of the probe. The addition sequence of the reagents: probe solution (1.0 μmol/L), PBS buffer solution (pH 6.8, 7.0, 7.2, 7.4, 7.6 and 7.8) and KF (1.0 μmol/L).

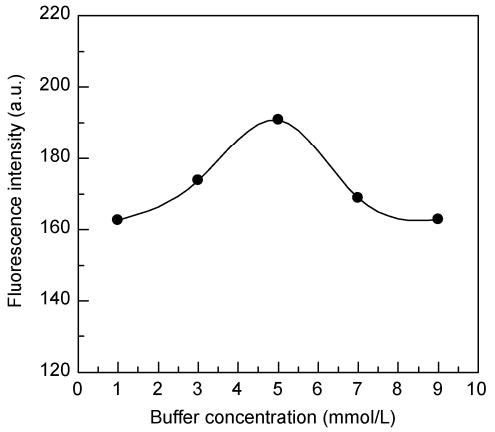

Figure 3 The effect of the PBS concentration on the fluorescence intensity of the probe. The addition sequence of the reagents: probe solution (1.0 μmol/L), PBS buffer solution (pH 7.4, 1.0, 3.0, 5.0, 7.0 and 9.0 mmol/L) and KF (1.0 μmol/L).

2.3 Optical responses to F^-

When BODIPY-Se (1.0 μmol/L) reacted with F^- at different concentrations, good linearity was observed between the fluorescence intensity and the concentration of F^- over the range of 0.10 to 1.0 μmol/L (Figures 5 and 6). The regression equation was $F = 118.12 + 72.23\ [F^-]$ (10^{-6} mol/L), with a linear coefficient efficient of 0.9918. The detection limit was 7.4×10^{-8} mol/L.

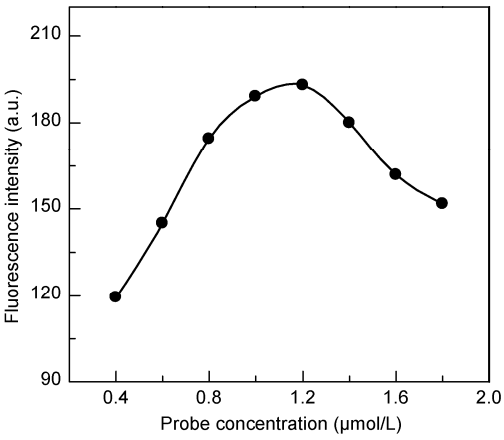

Figure 4 The effect of the probe concentration on the fluorescence intensity of the probe. The addition sequence of the reagents: Probe solution (0.4, 0.6, 0.8, 1.0, 1.2, 1.4, 1.6 and 1.8 μmol/L), PBS buffer solution (pH 7.4, 5.0 mmol/L) and KF (1.0 μmol/L).

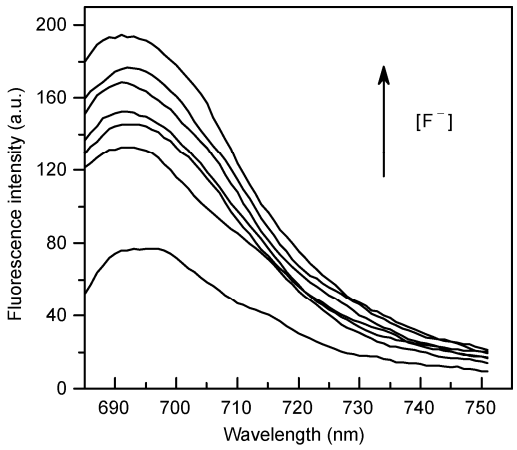

Figure 5 Emission spectra of BODIPY-Se after reacting with F^- at different concentrations. The addition sequence of the reagents: probe solution (1.0 μmol/L), PBS buffer solution (pH 7.4, 5.0 mmol/L) and KF (0.10, 0.40, 0.50, 0.70, 0.80, 1.0 μmol/L).

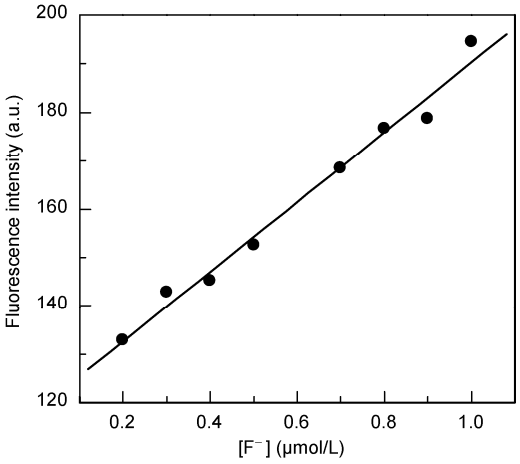

Figure 6 The linear relation between fluorescence intensity and the concentration of F^- in the range of 0.10 to 1.0 μmol/L.

2.4 Evaluation of the selectivity of the probe

On account of the complexity of the intracellular environment, we examined whether other anions could potentially interfere with the F^- measurements. BODIPY-Se showed a strong response toward F^- and negligible responses toward other anions ($C_2O_4^{2-}$, NO_2^-, NO_3^-, I^-, HCO_3^-, Br^-, CO_3^{2-}, Cl^-, CN^-, SO_4^{2-}) (Figure 7). Therefore, this probe can detect intracellular F^- without interference from other biologically relevant analytes.

2.5 Kinetic assay

A kinetic assay of the probe was performed. As shown in Figure 8, the probe reacted with F^- in 30 min and the fluorescent intensity was stable after 50 min. These results demonstrate that the probe is stable in solution and completely reacts with F^- in ~30 min. The fluorescent intensity was stable after 50 min.

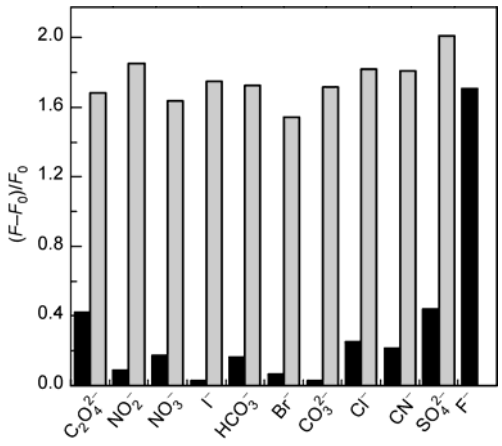

Figure 7 Fluorescence responses of BODIPY-Se toward F^- and other anions. Black bars represent the addition of the fluorine ion (1.0 μmol/L) or other anions (1.0 mmol/L) to the BODIPY-Se solution (1.0 μmol/L). Grey bars represent the addition of the fluorine ion (1.0 μmol/L) plus other anions (1.0 mmol/L) to the BODIPY-Se solution (1.0 μmol/L).

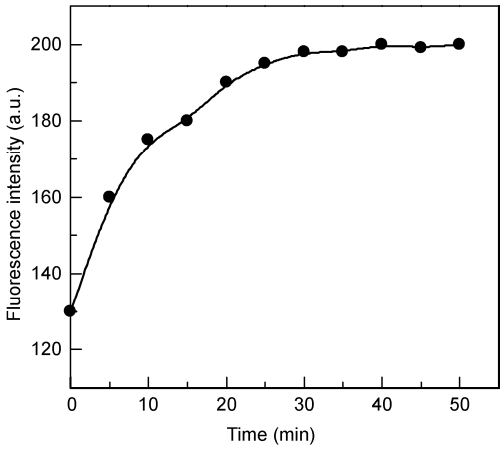

Figure 8 Time course of the fluorescence response of BODIPY-Se to F^-. The addition sequence of the reagents: probe solution (1.0 μmol/L), PBS buffer solution (pH 7.4, 5.0 mmol/L) and KF (1.0 μmol/L).

2.6 Confocal imaging

To test the capability of BODIPY-Se in imaging F^- in living cells, BODIPY-Se was added to human hepatoma cells (HepG2). After incubation with BODIPY-Se (1.0 μmol/L) for 1 h, HepG2 cells showed weak fluorescence. However, when incubated with F^- (1.0 μmol/L) for 1 h, and then incubated with the probe (1.0 μmol/L) for 1 h, HepG2 cells showed a clear increase in the intracellular fluorescence intensity (Figure 9). The bright-field images confirmed that the cells were viable throughout the imaging experiments. The results clearly demonstrated that BODIPY-Se was able to sense the differences in F^- concentrations in HepG2 cells. Confocal microscopic imaging of HepG2 cells reveals that the probe is cell-permeable and responsive toward intracellular F^-.

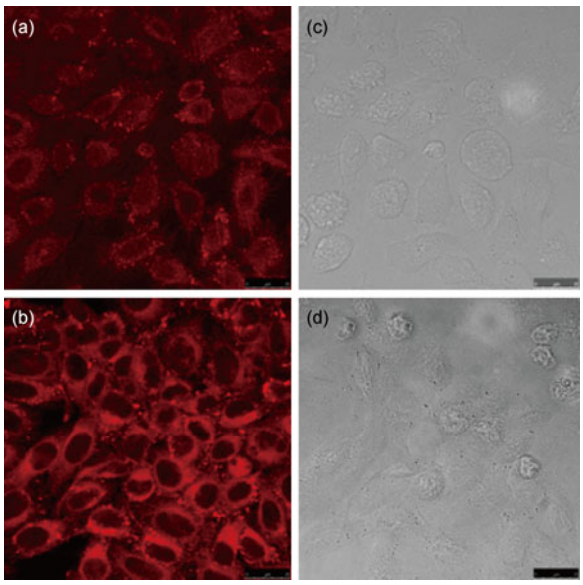

Figure 9 Confocal fluorescence images of living HepG2 cells. (a) Incubated with the probe (1.0 μmol/L) for 1 h; (b) incubated with F^- (1.0 μmol/L) for 1 h and then incubated with the probe (1.0 μmol/L) for 1 h; (c) and (d) represent the bright field images of (a) and (b), respectively.

3 Conclusions

In this report, we have designed and synthesized a novel fluorescent probe (BODIPY-Se) based on a Se-B bond. Selective detection of F^- in the near infrared range was realized because of the strong nucleophilicity of F^-. Good linearity between fluorescence intensity and the concentration of F^- was observed, and the limit of detection of the method reached 7.4×10^{-8} mol/L. Real-time imaging of F^- in living cells was also successfully achieved. This probe should be suitable for the detection and quantification of F^- in biological systems.

This work was supported by the National Basic Research Program of China (2007CB936000), the National Natural Science Foundation of China (20875057), the National Natural Science Funds for Distinguished Young Scholar (20725518), the National Key Natural Science Foundation of China (21035003), the Science and Technology Development Programs of Shandong Province of China (2008GG30003012) and the Key Natural Science Foundation of Shandong Province of China (ZR2010BZ001).

1 Briancon D. Fluoride and osteoporosis: An overview. Rev Rhum Engl Ed, 1997, 64: 78–81
2 Kleerekoper M. The role of fluoride in the prevention of osteoporosis. Endocrinol Metab Clin, 1998, 27: 441–452
3 Kissa E. Determination of inorganic fluoride in blood with a fluoride ion-selective electrode. Clin Chem, 1987, 33: 253–255
4 Kirk K L. Biochemistry of the Halogens and Inorganic Halides. New York: Plenum Press, 1991
5 Emmanuele D V, Thomas U, Rosario R, et al. Phenylmethanesulfonyl fluoride inactivates an archaeal superoxide dismutase by chemical modification of a specific tyrosine residue. Eur J Biochem, 2001, 268: 1794–1801
6 Mullenix P J, Denbesten P K, Schunior A, et al. Neurotoxicity of sodium fluoride in rats. Neurotoxicol Teratol, 1995, 17: 169–177
7 Katarzyna P G, Maria W, Wladyslaw W, et al. The role of fluoride ions in glycosaminoglycans sulphation in cultured fibroblasts. Fluoride, 1998, 31: 193–202
8 Zhao Y P, Zhao C C, Wu L Z, et al. First fluorescent sensor for fluoride based on 2-ureido-4[1*H*]-pyrimidinone quadruple hydrogen-bonded AADD supramolecular assembly. J Org Chem, 2006, 71: 2143–2146
9 Salvatore C, Philip A. Fluoride recognition in "super-extended cavity" calix[4]pyrroles. Chem Commun, 2000, 13: 1129–1130
10 Toni N, Yvonne D, Thomas B. Highly sensitive sensory materials for fluoride ions based on the dithieno [3,2-*b*:2',3'-*d*]phosphole system. Org Lett, 2006, 8: 495–497
11 Swamy K M, Lee Y J, Lee H N, et al. A new fluorescein derivative bearing a boronic acid group as a fluorescent chemosensor for fluoride ion. J Org Chem, 2006, 71: 8626–8628
12 Yamamoto H, Ori A, Ueda K, et al. Visual sensing of fluoride ion and saccharides utilizing a coupled redox reaction of ferrocenylboronic acids and dye molecules. Chem Commun, 1996, 3: 407–408
13 Kubo K, Kobayashi A, Ishida T, et al. Detection of anions using a fluorescent alizarin-phenylboronic acid ensemble. Chem Commun, 2005, 22: 2846–2848
14 Arimori S, Davidson M G, Fyles T M, et al. Synthesis and structural characterization of the first bis(bora)calixarene: A selective, bidentate, fluorescent fluoride sensor. Chem Commun, 2004, 14: 1640–1641
15 Paugam M F, Smith B D. Active transport of uridine through a liquid organic membrane mediated by phenylboronic acid and driven by a fluoride ion gradient. Tetrahedron Lett, 1993, 34: 3723–3726
16 Liu Z Q, Shi M, Li F Y, et al. Highly selective two-photon chemosensors for fluoride derived from organic boranes. Org Lett, 2005, 7: 5481–5484
17 Yamaguchi S, Akiyama S, Tamao K. Colorimetric fluoride ion sensing by boron-containing π-electron systems. J Am Chem Soc, 2001, 123: 11372–11375
18 Dusemund C, Sandanayake K R A S, Shinkai S. Selective fluoride recognition with ferroceneboronic acid. Chem Commun, 1995, 3: 333–334
19 Cooper C R, Spencer N, James T D. Selective fluorescence detection of fluoride using boronic acids. Chem Commun, 1998, 13: 1365–1366
20 Descalzo A B, Jim´enez D, Haskouri J E, et al. A new method for fluoride determination by using fluorophores and dyes anchored onto MCM-41. Chem Commun, 2002, 6: 562–563
21 Zhu C Q, Chen J L, Zheng H, et al. A colorimetric method for fluoride determination in aqueous samples based on the hydroxyl deprotection reaction of a cyanine dye. Anal Chim Acta, 2005, 539: 311–316
22 Yang X F , Ye S J, Bai Q, et al. A fluorescein-based fluorogenic probe for fluoride ion based on the fluoride-induced cleavage of *tert*-butyldimethylsilyl ether. J Fluoresc, 2007, 17: 81–87
23 Yamaguchi S, Akiyama S, Tamao K. Photophysical properties changes caused by hypercoordination of organosilicon compounds: From trianthrylfluorosilane to trianthryldifluorosilicate. J Am Chem Soc, 2000, 122: 6793–6794
24 Ikeda C, Maruyama T, Nabeshima T. Convenient and highly efficient synthesis of boron-dipyrrins bearing an arylboronate center. Tetrahedron Lett, 2009, 50: 3349–3351
25 Tahtaoui C, Thomas C, Rohmer F, et al. Convenient method to access new 4,4-dialkoxy and 4,4-diaryloxy-diaza-s-indacene dyes: Synthesis and spectroscopic evaluation. J Org Chem, 2007, 72: 269–272
26 Goeb S, Ziessel R. Convenient synthesis of green diisoindolodithienylpyrromethene-dialkynyl borane dyes. Org Lett, 2007, 9: 737–740
27 Ulrich G, Goze C, Goeb S, et al. New fluorescent aryl- or ethynylarylboron-substituted indacenes as promising dyes. New J Chem, 2006, 30: 982–986